ChemComm

Accepted Manuscript

This article can be cited before page numbers have been issued, to do this please use: A. K. Sharma, H. Singh and H. Chakrapani, *Chem. Commun.*, 2019, DOI: 10.1039/C9CC01747J.

ROYAL SOCIETY OF CHEMISTRY

rsc.li/chemcomm

ROYAL SOCIETY OF CHEMISTRY View Article Online
DOI: 10.1039/C9CC01747J

Journal Name

COMMUNICATION

Photocontrolled Endogenous Reactive Oxygen Species (ROS) Generation

Ajay Kumar Sharma,[a] Harshit Singh[a] and Harinath Chakrapani*,[a]

Received 00th January 20xx,
Accepted 00th January 20xx

DOI: 10.1039/x0xx00000x

www.rsc.org/

A cell-permeable small molecule for light-triggered generation of endogenous reactive oxygen species (ROS) is reported.

Oxygen and its reduced forms such as superoxide ($O_2^{\bullet-}$), hydrogen peroxide (H_2O_2) and hydroxyl radical are generated during normal functioning of cells.[1] A number of intrinsic mechanisms have evolved to attenuate these reactive oxygen species (ROS).[2,3] Elevated ROS generated in cells are associated with numerous pathophysiological conditions including cancer, inflammation, diabetes and several neurodegenerative disorders.[4–6] ROS is also deployed in immune response to counter pathogens.[7] Elevation of endogenous ROS has been associated with inhibition of cancer growth both *in vitro* as well as in animal models.[8–12] For example, piperlongumine has been shown to enhance ROS within cells[13–18] but the precise mechanism by which this happens is yet unclear and would be critical to determine. Due to its short life, $O_2^{\bullet-}$ must be produced *in situ* by reaction with oxygen and electron donor.[19] Either small organic molecules that spontaneously react with oxygen or enzymatic methods that turnover a substrate to generate $O_2^{\bullet-}$ are frequently used. A combination of hypoxanthine and xanthine oxidase (X + XO) where hypoxanthine is metabolized by XO to produce $O_2^{\bullet-}$, predominantly produces $O_2^{\bullet-}$ in the proximity of cells. Any $O_2^{\bullet-}$ that is produced must diffuse across a lipid bilayer to exert its effects. However, $O_2^{\bullet-}$ is not highly permeable at neutral pH and hence, this protocol and other small-molecule based methods may not be useful for enhancing intracellular ROS. A number of bioreductively-activated ROS generators are known and these have been evaluated previously for their cancer therapeutic potential.[20–23] Although triggered by a bioreductive enzyme, these compounds have little spatiotemporal control over ROS production. The quaternary amine, paraquat or menadione, which require bioactivation for $O_2^{\bullet-}$ production,[20,21] have often been used but at elevated concentrations that can potentially complicate mechanistic interpretations. Furthermore, their reactivity with biological thiols leading to covalent modification is also a major concern. Hartley and coworkers have developed a mitochondria-specific ROS generator, MitoPQ, a paraquat derivative.[24] This strategy allows for organelle-specific generation of ROS. Since light as a tool for activation offers spatiotemporal control,[25–33] photocleavable ROS generators are expected to have significant advantages. Chang and co-workers have reported a light-triggerable ROS generator that is based on hydroxyquinol.[30] This compound responds to light of wavelength of 305 nm, which is not desirable. Furthermore, the yield of hydrogen peroxide from this compound was somewhat diminished. Here, we report the design, synthesis and evaluation of a light-triggered endogenous ROS generator.

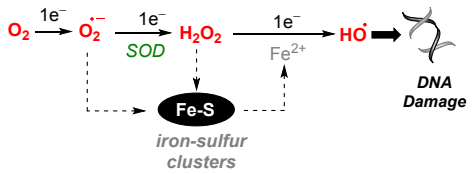

Figure 1. Endogenous ROS and some of their effects within cells.

Our laboratory has previously reported **1**,[34] which is a derivative of juglone, as a ROS generator (Scheme 1). The proposed mechanism for ROS generation was enolization of the carbonyl as the first step, followed by generation of a 1,4-diol. The diolate of this is electron-rich and is known to produce superoxide. We found that attaching a 4-nitrobenzyl group resulted in diminished ROS generation.[35] When triggered by nitroreductase, an enzyme that is present in bacteria, we found enhanced ROS generation.[35] Thus, this strategy enabled triggerable and localization of ROS production.[36] Recently, we reported an esterase-activated ROS generator that was able to elevate ROS within mammalian cells (Scheme 1).[36] Here, we report the design, synthesis and evaluation of a light-triggerable ROS generator.

[a] *Department of Chemistry, Indian Institute of Science Education and Research Pune. Pune 411 008. Maharashtra, India.*
† Footnotes relating to the title and/or authors should appear here.
Electronic Supplementary Information (ESI) available: [details of any supplementary information available should be included here]. See DOI: 10.1039/x0xx00000x

View Article Online
DOI: 10.1039/C9CC01747J

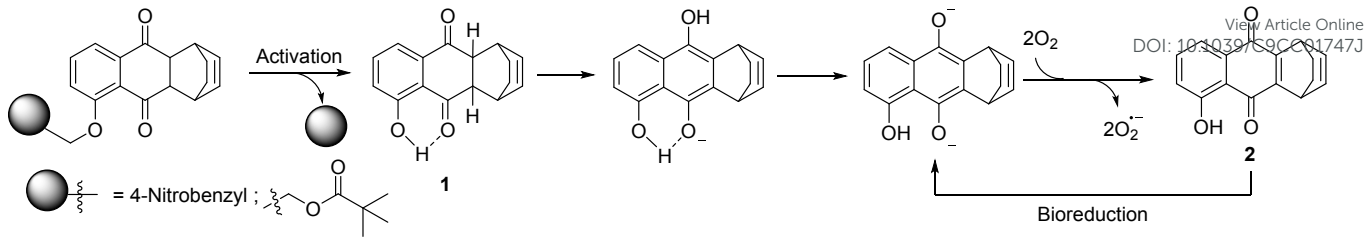

Scheme 1. General strategy for generation of compound **1** after photocleavage. Compound **1** generates superoxide during incubation in buffer under ambient aerobic conditions to produce the quinone **2**, which can further generate ROS through redox cycling. The 4-nitrobenzyl derivative is a substrate for nitroreductase while the pivaloyloxymethyl compound is triggered by esterase. The proposed substrate for photocleavage has a 2-nitroaryl functional group, which is expected to undergo deprotection to produce the ROS generator **1** (See Table 1).

The 2-nitrobenzyl functional group has been widely used as a protective group for alcohols.[26–28,37] Upon irradiation, this photo-cleavable group releases an alcohol (Scheme 1). This strategy has been used by Chang and co-workers to release the 1,4-diol.[30] The yields of ROS were low possibly due to the poor efficiency of cleavage, and perhaps, low ROS generating capability. Lastly, aqueous solubility and cancer cell uptake may play a major role in determining the efficiency of ROS generation within cells. Thus, the ROS generator must have a synthetic handle to incorporate additional functional groups (such as biotin).[38–40]

Table 1. Reaction of bromides with **1**

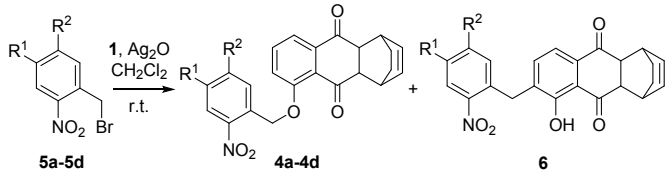

Entry	Bromide	R	R'	Prod	Yield
1	**5a**	H	H	**4a**	55%
2	**5b**	OMe	OMe	**4b** & **6**	30% & 11%
3	**5c**	OMe	O-Propargyl	**4c**	-
4	**5d**	OMe	$OCH_2CH_2N_3$	**4d**	25%

The bromides **5a**-**5b** were commercially obtained and independently reacted with **1**, resulting into the formation of compounds **4a** and **4b** (Table 1, entries 1-2). In the case of the reaction of the dimethoxy electrophile **5b**, the formation of the *C*-alkylated product (**6**) was observed. It is likely that a phenolate intermediate is formed, which can then react via the oxygen or the carbon to produce the *O*-alkylated or *C*-alkylated products. We next synthesized the bromide **5c**, which has a propargyl group on it. This alkyne should provide opportunities to conjugate biotin through the copper-catalyzed alkyne-azide click reaction. However, under the conditions that we used, we found no reaction between **5c** and **1** (Table 1, entry 3). Activation of the bromide by silver ions is an important step in the substitution reaction. It is likely that the alkyne coordinates with the silver ions and competes with activation of the bromide. We therefore revised our strategy and we first synthesized the bromide **5d**, which has an azide that can be utilized for orthogonal conjugation (Scheme S1 in ESI) and this was reacted with **1** and gave the corresponding azide **4d** in 25% yield. The desired conjugate **4e** was next synthesized by reacting **4d** with the biotin-alkyne derivative **12** (Figure 2A and Scheme S2 in ESI).

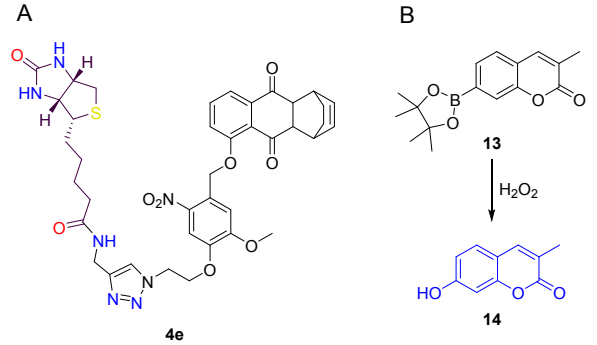

Figure 2. A) Structure of Biotinylated adduct **4e** B) Reaction of hydrogen peroxide with coumarin Boronate-ester dye **13**. The boronate ester **13** is weakly fluorescent and upon oxidation, a turn on fluorescence is observed due to the formation of **14**.

Next, the stability of the derivatives was evaluated. In the dark, we found no evidence for decomposition of these compounds in pH 7.4 buffer. To evaluate the photocleavage efficiency, **4a**, **4b** and **4e** were irradiated with 365 nm light and HPLC analysis revealed complete cleavage within 15 min. This cleavage resulted in the formation of **1**, a known ROS generator (Figure 3A, figure S2 in ESI). As previously reported, **1**, reacts with oxygen and produces $O_2^{\bullet-}$ which disproportionates to form H_2O_2,[34] another ROS. To validate the generation of $O_2^{\bullet-}$ during incubation of **4e**, this compound was irradiated and a dihydroethidium (DHE, see ESI) assay was used. The DHE dye reacts with $O_2^{\bullet-}$ and other ROS (H_2O_2, $\dot{O}H$) to form 2-hydroxy ethidium(2-OH-E^+) and ethidium (E^+) respectively (Scheme S4 in ESI), which can be detected by HPLC analysis.[41] When incubated, **4e** in the presence of light, under the assay conditions HPLC analysis revealed a peak at 29.5 min, which corresponds to 2-hydroxy ethidium (2-OH-E^+). This signal diminished when solution was treated with superoxide dismutase, a known quencher of $O_2^{\bullet-}$. When this experiment was conducted in the dark, no peak for 2-OH-E^+ was observed (Figure 3B). This data supports the generation of $O_2^{\bullet-}$ by **4e** only in the presence of light. This assay was also performed with **4a** and **4b** and similar results were obtained (Figure S3 in ESI).

The radical anion, $O_2^{\bullet-}$ disproportionates to form H_2O_2. We next assessed the production of H_2O_2 using two independent assays. First, the oxidation of fluorogenic boronic acids/esters has been frequently used to detect the presence of hydrogen

peroxide.[42,43] The non-fluorescent coumarin based dye **13** reacts with H_2O_2 to form umbelliferone derivative **14**, a highly fluorescent molecule (Figure 2B).

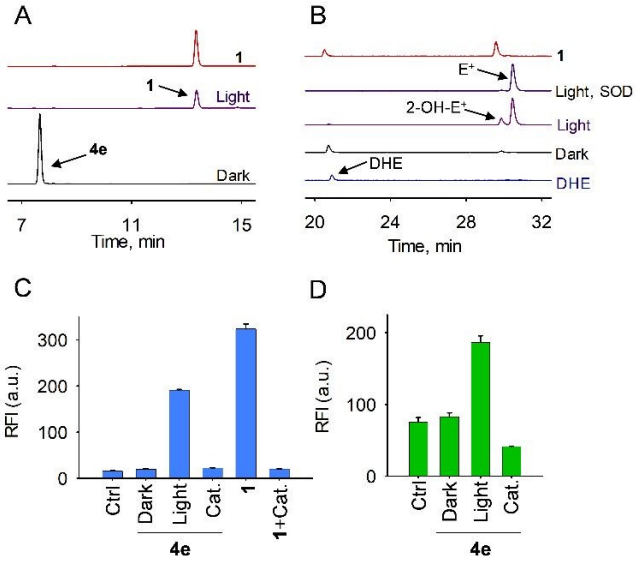

Figure 3. Photolysis and ROS analysis of **4e**; A) HPLC traces of **4e** (50 µM) in the presence and absence of Light, Light irradiation was performed by 365 nm light for 15 min with the 30 mW/cm² intensity. B) HPLC traces of DHE assay for superoxide detection, **4e** (25 µm) was irradiated with 30 mW/cm² 365 nm light for 15 min followed by addition of DHE and incubated for 1 h, as a control, SOD was used for quenching the superoxide; C) Hydrogen peroxide detection using dye the coumarin-boronate ester **13** as a probe. (excitation 320 nm; emission 460 nm); D) Hydrogen peroxide detection using Amplex red assay, **4e** (25 µM) was irradiated in 365 nm light for 15 min and incubated for 2 h, (cat.= Catalase enzyme). Data represent the mean±s.d. for 3 technical replicates per group.

Irradiated and non-irradiated samples of **4e** were independently incubated with dye **13** and fluorescence enhancement was found only with the irradiated sample (Figure 3C). This fluorescence signal was diminished in the presence of catalase, a known quencher of H_2O_2. This study was also performed with compounds **4a** and **4b** and as expected, fluorescence enhancement was observed in irradiated samples (Figure S4 in ESI). These results suggest that the production of H_2O_2 by **4e** occurred only in the presence of light. Next, an Amplex Red assay was used to infer the production of H_2O_2. Again, irradiated and non-irradiated samples of **4e** were independently treated with Amplex Red solution containing horse reddish peroxidase (HRP) enzyme and found that enhanced fluorescence signal was observed only in the irradiated sample. This signal was diminished in the presence of catalase (Figure 3D). Taken together, our results support the ability of **4e** to undergo photocleavage to produce ROS.

Next, this compound was evaluated as an endogenous ROS generator in cells after activation with light. First, generation of extracellular H_2O_2 was assessed by coumarin based dye **13** and Amplex Red in lung carcinoma cell line, A549 cells and it was found that **4e** was able to generate H_2O_2 extracellularly only in the presence of light. However, no ROS enhancement was observed by cells only in the presence of light and cells treated with **4e** in dark (Figure 4A, Figure S5 in ESI).

Further evaluation of intracellular ROS was also done by a cell permeable weakly fluorescent ROS responsive dye, 2',7'-dichlorodihydrofluorescein diacetate (H_2DCF-DA), which upon reaction with ROS forms a highly florescent molecule, 2',7'-dichlorodihydrofluorescein (DCF) and fluorescence intensity of this can be measured in well plate reader. This assay was performed in A549 cells and it was found that cells treated with **4e** had enhanced ROS level in the presence of light when compared with a similar treatment in the dark (Figure 4B & 4C). In addition, ROS enhancement was not observed when cells without **4e** was irradiated, suggesting that 365 nm UV light alone does not enhance the ROS level in cells. This study suggests that **4e** is cell permeable and elevate the ROS level only after irradiation with light.

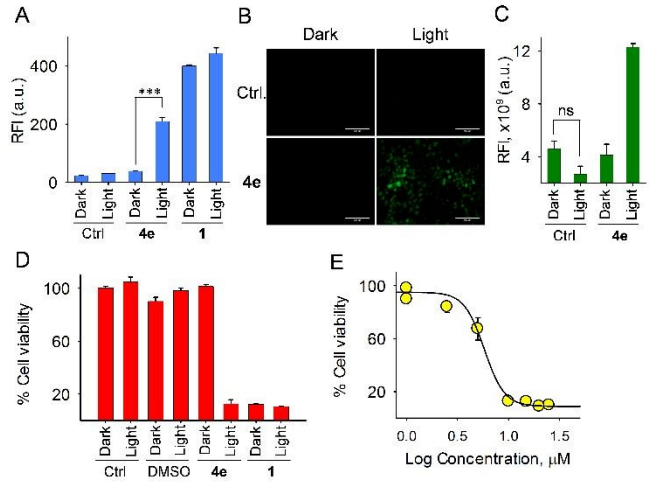

Figure 4. Cellular assays; A) Extracellular Hydrogen peroxide detection by Amplex red assay (excitation 550 nm; emission 590 nm; *** = p <0.0001); B & C) Intracellular ROS detection using H_2DCF-DA as a probe; Scale bar = 200 µm and ns = not significant. D) Cell viability assay using A549 cells with 10 µM compounds and E) Growth inhibition curve after irradiation with **4e** and IC_{50} was found to be 5.8 µM. Data represent the mean ± s.e.m. for 3 technical replicates per group.

Elevated levels of ROS can damage essential biomolecules leading to oxidative stress, which in turn can result in cell death. In order to test the hypothesis, cell viability assay was conducted using A549 and DLD-1 cell lines. Under the assay conditions, in the presence of **4e**, no significant inhibition of growth was observed in dark even at 50 µM (Figure S7 & S9 in ESI). When this experiment was conducted with cells that were irradiated (30 mW/cm² intense 365 nm light, 5 min), nearly complete inhibition of growth of these cells was observed at 10 µM (Figure 4D, Figure S8 in ESI). The inhibitory concentration 50% (IC_{50}) of **4e** in the presence of light was found to be 5.8 µM (Figure 4E). Similarly, in DLD-1 cells, no significant inhibition was observed in the dark while potent inhibitory effects were observed during irradiation (IC_{50} = 5.3 µM) (Figure S8-S9 in ESI).

Recently, the ROS generating capability of **1** was compared with various other probes. A major drawback of several ROS generators is the inherent reactivity with thiols. For example, menadione and Juglone reacts with glutathione (Figure S10D in ESI). However, with **1** and the oxidized form of **1**, i.e. **2**, we found no evidence for reaction with glutathione even after incubation for several hours (Figure S10 in ESI). The reason for negligible reactivity with glutathione might be the absence of α, β-

unsaturated site in **1** whereas this site could be sterically inaccessible in **2**. Hence, this ROS generator has advantages over other ROS generators such as menadione since it allows us to study the effects of ROS without complications associated with covalent modification. Furthermore, the improved aqueous solubility of **4e** presents opportunities for wide applicability of this compound as a ROS generator.

Taken together, our results suggest the use of the compound for photolabile "turn on" ROS generation and overexpression of biotin receptors in cancer cells may provide an opportunity to selectively target tumour.[38–40] As a cancer therapeutic, singlet oxygen has been used;[44] however, examples of the use of other biological ROS are fewer.[45] The ability to conjugate this ROS generator with directing groups enhances the versatility of this tool.

This work was supported by the Department of Biotechnology, India (Grant number: BT/PR17514/BRB/10/1615/2017) and the Council for Scientific and Industrial Research (Fellowship). The authors thank Ms. Preeti Chauhan, IISER Pune for help with setting up cellular assays.

Conflicts of interest

There are no conflicts to declare.

Notes and references

1 M. Schieber and N. S. Chandel, *Curr. Biol.*, 2014, **24**, R453–R462.
2 S. B. Nimse and D. Pal, *RSC Adv.*, 2015, **5**, 27986–28006.
3 J.-M. Lü, P. H. Lin, Q. Yao and C. Chen, *J. Cell. Mol. Med.*, 2010, **14**, 840–860.
4 B. Uttara, A. Singh, P. Zamboni and R. Mahajan, *Curr. Neuropharmacol.*, 2009, **7**, 65–74.
5 Z. Liu, T. Zhou, A. C. Ziegler, P. Dimitrion and L. Zuo, *Oxid. Med. Cell. Longev.*, 2017, **2017**, 1–11.
6 G. H. Kim, J. E. Kim, S. J. Rhie and S. Yoon, *Exp. Neurobiol.*, 2015, **24**, 325.
7 Y. Yang, A. V. Bazhin, J. Werner and S. Karakhanova, *Int. Rev. Immunol.*, 2013, **32**, 249–270.
8 J. Wang and J. Yi, *Cancer Biol. Ther.*, 2008, **7**, 1875–84.
9 J. P. Fruehauf and F. L. Meyskens, *Clin. Cancer Res.*, 2007, **13**, 789–794.
10 S. Suzuki, M. Higuchi, R. J. Proske, N. Oridate, W. K. Hong and R. Lotan, *Oncogene*, 1999, **18**, 6380–6387.
11 D. J. Adams, Z. V. Boskovic, J. R. Theriault, A. J. Wang, A. M. Stern, B. K. Wagner, A. F. Shamji and S. L. Schreiber, *ACS Chem. Biol.*, 2013, **8**, 923–929.
12 A. T. Dharmaraja, *J. Med. Chem.*, 2017, **60**, 3221–3240.
13 J.-L. Roh, E. H. Kim, J. Y. Park, J. W. Kim, M. Kwon and B.-H. Lee, *Oncotarget*, 2014, **5**, 9227–9238.
14 K. Karki, E. Hedrick, R. Kasiappan, U.-H. Jin and S. Safe, *Cancer Prev. Res.*, 2017, **10**, 467–477.
15 H. Dhillon, S. Chikara and K. M. Reindl, *Toxicol. Reports*, 2014, **1**, 309–318.
16 X. Xu, X. Fang, J. Wang and H. Zhu, *Bioorg. Med. Chem. Lett.*, 2017, **27**, 1325–1328.
17 W.-J. Yan, Q. Wang, C.-H. Yuan, F. Wang, Y. Ji, F. Dai, X.-L. Jin and B. Zhou, *Free Radic. Biol. Med.*, 2016, **97**, 109–123.
18 L.-H. Gong, X.-X. Chen, H. Wang, Q.-W. Jiang, S.-S. Pan, J.-G. Qiu, X.-L. Mei, Y.-Q. Xue, W.-M. Qin, F.-Y. Zheng, Z. Shi and X.-J. Yan, *Oxid. Med. Cell. Longev.*, 2014, **2014**, 906804.
19 M. Hayyan, M. A. Hashim and I. M. AlNashef, *Chem. Rev.*, 2016, **116**, 3029–3085.
20 D. N. Criddle, S. Gillies, H. K. Baumgartner-Wilson, M. Jaffar, E. C. Chinje, S. Passmore, M. Chvanov, S. Barrow, O. V Gerasimenko, A. V Tepikin, R. Sutton and O. H. Petersen, *J. Biol. Chem.*, 2006, **281**, 40485–92.
21 D. M. Frank, P. K. Arora, J. L. Blumer and L. M. Sayre, *Biochem. Biophys. Res. Commun.*, 1987, **147**, 1095–1104.
22 V. S. Khodade, M. Sharath Chandra, A. Banerjee, S. Lahiri, M. Pulipeta, R. Rangarajan and H. Chakrapani, *ACS Med. Chem. Lett.*, 2014, **5**, 777–781.
23 M. A. Silvers, S. Deja, N. Singh, R. A. Egnatchik, J. Sudderth, X. Luo, M. S. Beg, S. C. Burgess, R. J. DeBerardinis, D. A. Boothman and M. E. Merritt, *J. Biol. Chem.*, 2017, **292**, 18203–18216.
24 E. L. Robb, J. M. Gawel, D. Aksentijević, H. M. Cochemé, T. S. Stewart, M. M. Shchepinova, H. Qiang, T. A. Prime, T. P. Bright, A. M. James, M. J. Shattock, H. M. Senn, R. C. Hartley and M. P. Murphy, *Free Radic. Biol. Med.*, 2015, **89**, 883–894.
25 P. Klán, T. Šolomek, C. G. Bochet, A. Blanc, R. Givens, M. Rubina, V. Popik, A. Kostikov and J. Wirz, *Chem. Rev.*, 2013, **113**, 119–191.
26 S. Chalmers, S. T. Caldwell, C. Quin, T. A. Prime, A. M. James, A. G. Cairns, M. P. Murphy, J. G. McCarron and R. C. Hartley, *J. Am. Chem. Soc.*, 2012, **134**, 758–761.
27 M. J. Hansen, W. A. Velema, M. M. Lerch, W. Szymanski and B. L. Feringa, *Chem. Soc. Rev*, 2015, **44**, 3358.
28 Y. V Il'ichev, M. A. Schwö and J. Wirz, *J. Am. Chem. Soc.*, 2004, **126**, 4581–4595.
29 A. K. Sharma, M. Nair, P. Chauhan, K. Gupta, D. K. Saini and H. Chakrapani, *Org. Lett.*, 2017, **19**, 4822–4825.
30 E. W. Miller, N. Taulet, C. S. Onak, E. J. New, J. K. Lanselle, G. S. Smelick and C. J. Chang, *J. Am. Chem. Soc.*, 2010, **132**, 17071–17073.
31 Y. Li, Y. Shu, M. Liang, X. Xie, X. Jiao, X. Wang and B. Tang, *Angew. Chemie Int. Ed.*, 2018, **57**, 12415–12419.
32 Y. Iwamoto, M. Kodera and Y. Hitomi, *Chem. Commun.*, 2015, **51**, 9539–9542.
33 X. Xie, J. Fan, M. Liang, Y. Li, X. Jiao, X. Wang and B. Tang, *Chem. Commun.*, 2017, **53**, 11941–11944.
34 A. T. Dharmaraja, M. Alvala, D. Sriram, P. Yogeeswari and H. Chakrapani, *Chem. Commun.*, 2012, **48**, 10325–10327.
35 A. T. Dharmaraja and H. Chakrapani, *Org. Lett.*, 2014, **16**, 398–401.
36 D. S. Kelkar, G. Ravikumar, N. Mehendale, S. Singh, A. Joshi, A. K. Sharma, A. Mhetre, A. Rajendran, H. Chakrapani and S. S. Kamat, *Nat. Chem. Biol.*, 2019, **15**, 169–178.
37 A. Patchornik, B. Amit and R. B. Woodward, *J. Am. Chem. Soc.*, 1970, **92**, 6333–6335.
38 S. Luo, V. S. Kansara, X. Zhu, N. K. Mandava, D. Pal and A. K. Mitra, *Mol. Pharm.*, 2006, **3**, 329–339.
39 W. X. Ren, J. Han, S. Uhm, Y. J. Jang, C. Kang, J.-H. Kim and J. S. Kim, *Chem. Commun.*, 2015, **51**, 10403–10418.
40 T. Kim, H. M. Jeon, H. T. Le, T. W. Kim, C. Kang and J. S. Kim, *Chem. Commun.*, 2014, **50**, 7690.
41 H. Zhao, J. Joseph, H. M. Fales, E. A. Sokoloski, R. L. Levine, J. Vasquez-Vivar and B. Kalyanaraman, *Proc. Natl. Acad. Sci. U. S. A.*, 2005, **102**, 5727–32.
42 E. W. Miller, A. E. Albers, A. Pralle, E. Y. Isacoff and C. J. Chang, *J. Am. Chem. Soc.*, 2005, **127**, 16652–16659.
43 V. S. Khodade, A. Kulkarni, A. Sen Gupta, K. Sengupta and H. Chakrapani, *Org. Lett.*, 2016, **18**, 1274–1277.
44 P. Agostinis, K. Berg, K. A. Cengel, T. H. Foster, A. W. Girotti, S. O. Gollnick, S. M. Hahn, M. R. Hamblin, A. Juzeniene, D. Kessel, M. Korbelik, J. Moan, P. Mroz, D. Nowis, J. Piette, B. C. Wilson and J. Golab, *CA. Cancer J. Clin.*, 2011, **61**, 250–81.
45 A. N. Onyango, *Oxid. Med. Cell. Longev.*, 2016, **2016**, 2398573.